Radiography 29 (2023) 705–711

Contents lists available at ScienceDirect

Radiography

journal homepage: www.elsevier.com/locate/radi

Technical and clinical assessment of latest technology SiPM integrated digital PETCT scanner

M.K. Singh [a], P. Mohan [b], H. Mahajan [b], C. Kaushik [c, *]

[a] Medikabazaar, Technopolis Knowledge Park, Mumbai, 400093, India
[b] Mahajan Imaging, Hauz Khas Enclave, New Delhi, 110016, India
[c] School of Health and Society, University of Salford, Manchester, M5 4WT, United Kingdom

ARTICLE INFO

Article history:
Received 2 February 2023
Received in revised form
5 April 2023
Accepted 26 April 2023

Keywords:
NEMA
PETCT
SiPM
LYSO

ABSTRACT

Objective: The aim of this study was to conduct a technical and clinical evaluation of a Silicon Photomultiplier (SiPM) integrated digital Positron Emission Tomography – Computed Tomography (PETCT) Scanner using National Electrical Manufacturers Association (NEMA) NU 2- 2018 standards.
Methods: System sensitivity was measured by using a NEMA sensitivity phantom. Scatter fraction, count-rate performance, accuracy of count loss, and timing resolution were all computed. Clinical images were acquired and image quality was assessed and compared with published studies.
Results: At 1 cm, tangential, radial, and axial spatial resolutions were 3.02 mm, 3.02 mm, and 2.73 mm at full width half maximum (FWHM), respectively. Sensitivity at centre and 10 cm was 10.359 cps/kBq and 9.741 cps/kBq, respectively. The timing resolution was measured at 372 ps.
Conclusion: The digital PETCT exhibits a high-spatial resolution and a superior timing resolution, which advances the diagnostic ability to detect small lesions and boosts the diagnostic confidence.
Implications for practice: Increases clinical relevance by improving the ability to detect and differentiate tiny or low-contrast lesions without compromising radiopharmaceutical dose or overall scan time.

Introduction

PET is fundamentally an imaging technology that measures physiological and metabolic uptake information in the human body.[1] Different suppliers use various detector and crystal technologies in their PET systems.[2] In digital PETCT, the standard PMT detector has been replaced with SiPM.[3–5] SiPM consumes significantly less power than PMTs.[3,4] Currently, various manufacturers use SiPM-based digital PET/CT systems in healthcare.[6] National Electrical Manufacturers Association (NEMA) NU 2-2018 is the most recent PET technical assessment guide, and it incorporates the measuring standard for evaluating the technical assessments.[6–9] Present technical report comprises the evaluation of technical assessment of uMI 550 digital PETCT. As per NEMA NU 2-2018, various performance test was conducted namely, sensitivity test, spatial resolution, scatter fraction, image quality of PET (IQ) test, NECR, timing resolution, accuracy of count loss and correction of random events in PET by using Fluorine 18-Sodium Fluoride (18F–NaF) radiopharmaceutical.[8,10]

Methodology

uMI 550 digital PETCT scanner

The UIH model uMI 550 digital PET/CT is developed with LYSO ($Lu^{1.8}Y^{.2}SiO^5$:Ce) crystals integrated with silicon photomultiplier (SiPM) detectors with axial-field of views (AFOVs) of 24 cm. On PET hardware aspects, one-unit structure consists of ~70 SiPM detectors, and one detector unit includes ~42 LYSO crystals array of ($2.76 \times 2.76 \times 16.3\ mm^3$) connected with SiPM detectors. As a result, each unit has axial coverage dimensions of 100 mm × 240 mm. In this digital PET scanner, a total of 22 units were assembled in a cylindrical configuration.

Technical and clinical assessment

The performance of a digital PET scanner was evaluated in accordance with the most recent NEMA NU 2-2018 standard.[6–8,10]

Abbreviations: NEMA, National Electrical Manufacturers Association; PETCT, Positron Emission Tomography Computed Tomography; SiPM, Silicon Photomultiplier; LYSO, Lutetium–yttrium oxyorthosilicate.

* Corresponding author.
E-mail addresses: C.Kaushik@salford.ac.uk, drchanchalkaushik13@gmail.com (C. Kaushik).

https://doi.org/10.1016/j.radi.2023.04.020

The system's evaluations included spatial resolution, NEMA sensitivity, ToF sensitivity, count loss accuracy, scatter fraction, timing resolution, count rate performance (NECR), random event corrections, and PET image quality.

Spatial resolution

According to NEMA, a 18F—NaF point source is employed to estimate spatial resolution.[8,10] The spatial resolution was estimated in two halves, the first at half AFOV and the second at 1/8th AFOV. Within each section plane, the resolution was computed at 1 cm and 10 cm intervals. The 18F—NaF point source, with an activity of 0.74 megabecquerel (MBq), was produced in-house according to the manufacturer's specifications. A total of 5 million net true counts were acquired for each computing position, and the counts were subsequently processed by an internal control acquisition system. For the image reconstruction, a ramp filter was utilized in conjunction with the default configuration technique of filtered back projection to obtain all the images (inbuild control acquisition system).

Sensitivity

The sensitivity test was performed using a phantom, which is made up of five concentric sheaths of aluminum with a standard length of 70 cm. By filling a polyethylene tube with 18F—NaF solution, a 700 mm long tube line source was created. At the time of the scan, the activity was ~15 MBq. The line source was put into the aluminum sheath while held parallel to the axis of the PET scanner. The phantom was placed in two locations: in the centre of the AFOV and 10 cm away from it. According to the manufacturer's protocol, five-minute scans were performed at each fixed location, followed by the addition of an aluminum sheath. A delayed coincidence window was also set up to eliminate random coincidence events during acquisition.

Count losses, scatter fraction, and randoms fraction

A phantom measuring 70 cm long and 20 cm in diameter was used to assess the count losses, scatter fraction, and random fraction on this PET scanner. The radioactivity of a filled line source with 500 MBq (18F—NaF, 10% range) was ~700 mm long. The line source was 45 mm distant from the centre of the phantom and parallel to its axis. The activity-filled phantom's position on the scanning table assured that the line source was directed downward. After positioning the phantom-filled activity source, the scan commenced. This acquisition's scan protocol was 34 timing frames, which took 11 h to complete, and the test was executed overnight. Following completion of the acquisition in list mode and utilizing the manufacturer's protocol in the acquisition system, total, true, scatter, random, and noise equivalent count rates were evaluated in accordance with NEMA NU2-2018, and an automated graph showing the results was generated.

Accuracy of random and count loss corrections

The raw list mode PET data was reconstructed in order to compute the accuracy of count loss and random corrections. The randoms were chosen by establishing a delayed coincidence window, and the scatter photons were assessed using the Monte-Carlo method. The manufacturer's standard methodology was used to obtain 85 image slices with a slice thickness of 2.85 mm using TOF, point spread function (PSF), and ordered subsets expectation maximization (OSEM) reconstruction.

Image quality

A body phantom was used to examine image quality. The phantom's core was filled with six different-sized spheres packed with 18F—NaF radioactivity, each measuring 10, 13, 17, 22, 28, and 37 mm in diameter. All sphere centre shares the same axial plane. The backdrop portion of this phantom had a capacity of 9.8 L (L) and was charged with an 18F—NaF solution containing less than 5 kilobecquerel per milliliter (KBq/mL) of radioactivity. In spheres, the concentration of 18F—NaF radioactivity was four times higher than the background section activity. A line source comprising 18F— NaF and 120 MBq was also put inside the scatter phantom during acquisition. For this phantom scan, a duration of 5 min per bed position was used to minimize a 100 cm long scanning distance to roughly 30 min with 50% bed overlap during acquisition as per the default procedure. The CT attenuation map was used to compensate attenuation in PET images. PET reconstruction with TOF and PSF-OSEM reconstruction yielded a total of 85 image slices. Each hot sphere had a circular ROI drawn upon it by manually, and same size ROI was applied on all hot spheres.

The ROI average counts (Cs) for each sphere were computed. The ROIs for the hot sphere were then replicated and pasted in identical sizes into the background section of image slices. The average counts for each background ROI (CB) were also obtained. The contrast recovery coefficients (CRC) of the 18F—NaF concentration filled in spheres and the background section were calculated. Furthermore, CRC and background were evaluated for all spheres, as well as the relative error in the lung equivalent insert, in compliance with the NEMA standard, utilizing the average count values for each ROI.

Timing resolution

After altering the scatter, random, and off-center positions of the phantom (line source fitted), the timing resolution was calculated using the full width half maximum (FWHM) and full width tenth maximum (FWTM) of the temporal distribution of coincident events.

CT component

uMI550 digital PETCT has been integrated with 40 physical detector rows. Each detector size was 0.55 mm and the overall width of the detector was 22 mm. The measured low contrast resolution was 3 mm at 1% contrast and the high contrast resolution was 10.0 lp/cm.

Results

Spatial resolution

Tangential, radial, and axial spatial resolutions with FWHM values at 1 cm radial offset were evaluated as 3.02 mm, 3.02 mm, and 2.73 mm, respectively. The resolutions slightly decreased at 10 cm radial offset to 3.09 mm, 3.43 mm, and 2.98 mm, respectively, and further diminished at 20 cm radial offset to 3.62 mm, 4.65 mm, and 3.17 mm, respectively (Table 1). Tangential, radial, and axial spatial resolutions with FWTMs values at 1 cm radial offset were determined as 5.60 mm, 5.35 mm, and 5.54 mm FWTMs, respectively. The resolutions moderately deteriorated at 10 cm radial offset to 5.76 mm, 5.99 mm, and 5.75 mm respectively, and was further dropped at 20 cm radial offset to 6.09 mm, 8.03 mm, and 5.95 mm respectively (Table 1). The total NEMA sensitivity of the uMI 550 PET scanner was 10.359 cps/kBq at the centre and 9.741

Table 1
Average resolution over both axial position.

Source Location	(0,10)mm			(0,100)mm			(0,200)mm		
Direction	Tangential	Radial	Axial	Tangential	Radial	Axial	Tangential	Radial	Axial
FWHM (mm)	3.02	3.02	2.73	3.09	3.43	2.98	3.62	4.65	3.17
FWTM (mm)	5.6	5.35	5.54	5.76	5.99	5.75	6.09	8.03	5.95

cps/kBq at 10 cm offset. Fig. 1 (a, b) depicts the two axial sensitivity profiles of the 10 cm radial offset and the centre.

Assessment of the scatter fraction and count rate

Table 3 shows that at a clinically relevant activity concentration of 18F— NaF of 19.28 kBq/mL, a NEC rate of 130.05 kcps and a scatter fraction of 36.71% were computed. At peak NECR rate, the scatter fraction profile is 38.50%. Table 3 also shows that the peak NEC rate is 441.16 kcps at an activity concentration of 26.46 kBq/mL. Curves depict the count rates of NEC, prompts, trues, randoms, and scatter as they vary with radioactivity concentration (Fig. 1(f)).

Accuracy of random and count loss corrections

The count-rate errors at various activity concentrations are shown in Fig. 1 (c). The maximum and minimum count-rate relative errors at NECR peak were 1.55% and 1.38%, respectively.

Image quality

The aspect ratio of the sphere to the backdrop was 4:1, and the CRC of the heated spheres ranged from 50.5% (10 mm) to 84.5% (37 mm). The lung residual estimated was 5.6% (Fig. 1 d). Table 2 summarizes all CRCs and their related background variability. The

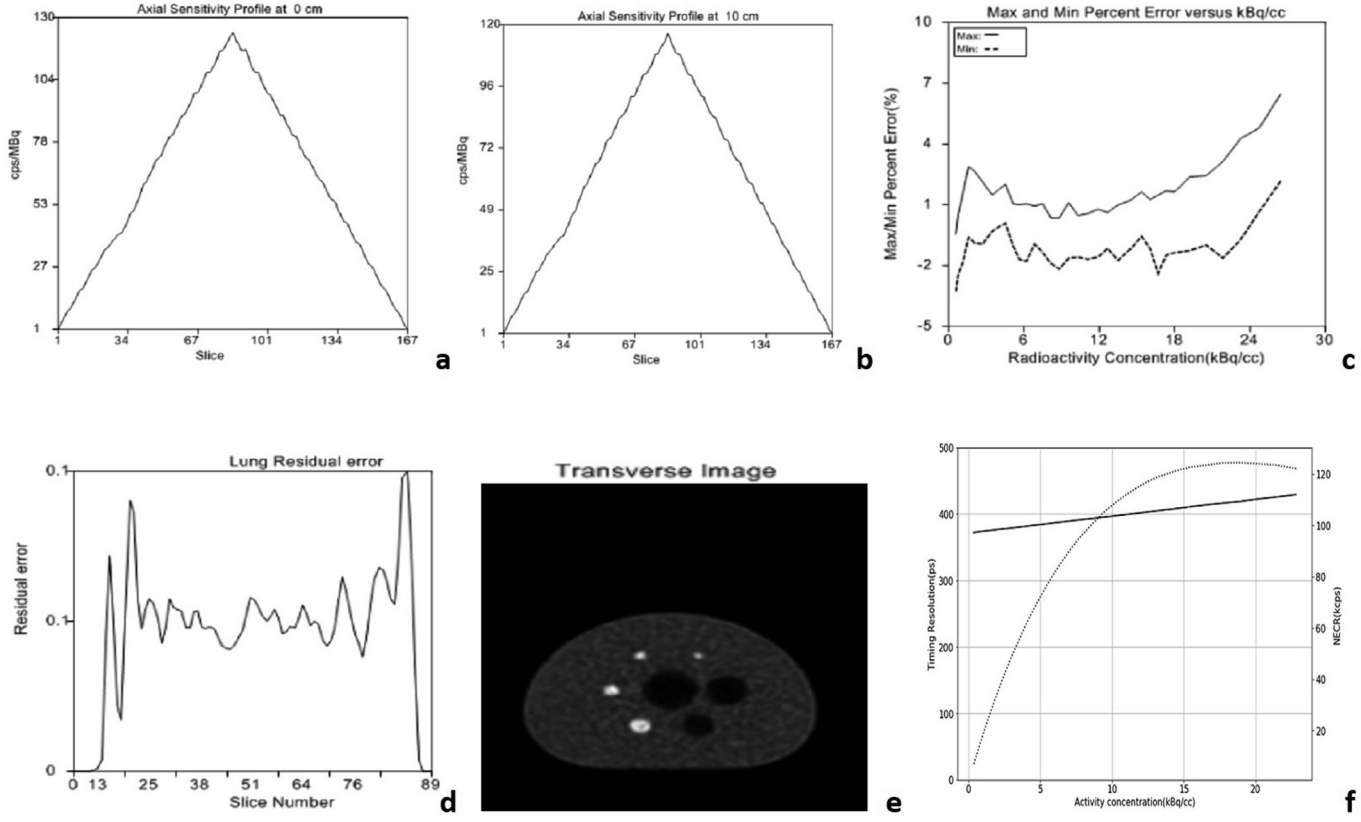

Figure 1. (a): System Sensitivity: 10.359 kcps/MBq, (b): System Sensitivity: 9.741 kcps/MBq (report values are calculated after the subtraction of randoms), (c,d): showing the central slice of the image quality phantom for the 4:1 measurement, (c) showing transverse image and (d) showing lung residual error, (e): Timing resolution curve (solid line) in dependency on activity concentration and also plotted NECR curve (dotted line) by using double Y axis.

Table 2
Summary of all CRCs and corresponding background variability.

Sphere Diameter (mm)		10	13	17	22	28	37	Lung Residual
Contrast Recovery (%)	Mean	50.5	62.3	74.7	81.6	82	84.5	NA
	Max	55.55	68.53	82.17	89.76	90.2	92.95	NA
	Min	45.45	56.07	67.23	73.44	73.8	76.05	NA
Background Variability (%)	Mean	6	4.8	3.9	3.3	2.7	2.2	5.6
	Max	6.6	5.28	4.29	3.63	2.97	2.42	5.04
	Min	5.4	4.32	3.51	2.97	2.43	1.98	6.16

Table 3
Analysis report for scatter fraction and count-rate performance.

System Scatter Fraction @peak NECR	38.50%
System Scatter Fraction @ low activity	36.71%
Peak True rate	441.16(kcps) @26.46(kBq/cc)
Peak NECR	130.05(kcps) @19.28(kBq/cc)
The Max % error below the NECR peak activity	3.24%

core slice of the picture quality phantom utilized in the 4:1 ratio computation is shown in Fig. 1 (e).

Timing resolution

Fig. 1(f) shows the timing resolution of 372 ps (ps) obtained at a low count-rate.

Comparison with similar AFOV PET scanners

The NEMA performance parameters of the uMI550 were compared to similar AFOV PET models (24–26 cm) of traditional analog and digital PET scanners integrated with CT and MRI modalities. This comparison has included United Imaging Healthcare (UIH) similar model digital PETCT and analog PETCT, GE healthcare analog PETCT, Digital PETCT and PETMRI, and Siemens Healthineers Digital PETCT and PETMRI (as shown in the Table 4).

Discussion

The technical evaluation of uMI550 was performed as per NEMA NU 2-2018.[6–8,10] The NEMA technical parameters were directly compared to similar AFOV PET scanners systems (analog and digital) integrated with either CT or MRI. In this study, seven PET scanner systems with an AFOV range of 24 cm–26 cm were compared as shown in Table 4.

AFOV

The AFOVs of the uMI550 PETCT system and the analog uMI510 PETCT scanner were 24 cm and 23.6 cm respectively. Siemens Healthineer Biograph vision 600 digital PETCT has an AFOV of 26.3 cm and its PETMRI Biograph mMR contained an AFOV of 25.8 cm. The AFOVs for GE healthcare scanners were 25 cm for analog PETCT Discovery IQ PETCT, Digital PETCT Discovery MI and Digital PETMRI Signa.[6,11–16]

Spatial resolution

The spatial resolution (tan/rad/axial) of uMI550 (Singh et al.) turned out to congruent with Chen et al. with percentage difference of 3.3%/0%/10.5% at 1 cm, 0%/2.98%/0% at 10 cm and 10.5%/11.4%/0% at 20 cm. The spatial resolution of the uMI550 PETCT system (Singh

Table 4
Comparison of NEMA technical parameters for PET scanners from different manufacturers.

Model	United Imaging uMI550	United Imaging uMI550[6]	United Imaging uMI510[11]	GE Discovery MI[12]	GE Discovery IQ[13]	GE Signa PET MR[14]	Siemens Biograph Vision 600[15]	Siemens Biograph mMR[16]
Authors	Singh et al., 2023	Chen et al., 2020	Xu et al., 2016	Pan et al., 2019	Llompart et al., 2017	Grant et al., 2016	Reddin et al., 2018	Delso et al., 2011
Manufacturer	United Imaging Healthcare	United Imaging Healthcare	United Imaging Healthcare	GE Healthcare	GE Healthcare	GE Healthcare	Siemens Healthineer	Siemens Healthineer
Specifications	NEMA NU 2-2018	NEMA NU 2-2018	NEMA NU 2-2007	NEMA NU 2-2012	NEMA NU 2-2012	NEMA NU 2-2012	NEMA NU 2-2018	NEMA NU 2-2007
AFOV (cm)	**24**	**24**	**23.6**	**25**	**25**	**25**	**26.3**	**25.8**
Crystal	LYSO	LYSO	LYSO	LYSO (LBS)	BGO	LYSO (LBS)	LSO	LSO
Detector	SiPM	SiPM	PMT	SiPM	PMT	SiPM	SiPM	APD
Crystal dimension (mm)	2.76 × 2.76 × 16.3	2.76 × 2.76 × 16.3	2.35 × 2.35 × 15	4 × 4 x 25	6.3 × 6.3 x 30	4.0 × 5.3 x 25	3.2 × 3.2 x 20	4 × 4 x 20
Spatial Resolution								
Tan/rad/axial @ 1 cm	3/3/2.7	2.9/3/3	2.85/3.0	4.3/4.3/5	4.7/4.2/4.8	4.1/4.4/5.3	3.7/3.5/3.6	4.3/4.3
Tan/rad/axial @ 10 cm	3/3.4/3	3/3.3/3	3/3.0	4.6/5.5/6.5	5.1/5.6/4.8	4.4/5.8/6.7	3.9/4.6/4.3	4.8/5.2/6.6
Tan/rad/axial @ 20 cm	3.6/4.6/3.1	4/4.1/3.1	NA	5/7.4/6.6	5.5/8.5/4.8	5.2/8.4/7.2	3.5/5.8/4.4	NA
Sensitivity (cps/kBq)								
Centre	10.35	10.24	8.3	20.81	20.8	23.3	15.1	15
10 cm	9.74	10.32	8.6	20.21	20.4	22.8	15.6	13.8
Count Rate								
Scatter fraction (%)	38.5	36.65	38.5	40.2	36.2	43.6	39	37.9
Peak NECR (kcps)	130.05(kcps) @19.28(kBq/cc)	124.4 kcps @ 18.85 kBq/mL	109 kcps @ 21.5 kBq/mL	266.3 kcps @ 20.8 kBq/ml	123.6 kcps @ 9.1 kBq/mL	218 kcps @17.8 kBq/mL	296 kcps @ 30.9 kBq/ml	184 kcps @23.1 kBq/mL
Timing Resolution (ps)	372	372	485	381.7	Non ToF	386	215	Non ToF
Image Quality (%)								
10 mm (CR/BV)	50.5/6	46.5/6.4	NA	46/9.3	18/4.4	35.2/4.9	86.8/6	32.5/5.3
13 mm (CR/BV)	62.3/4.8	76.2/5.5	NA	54/7.1	37/4	48.9/4.0	72.2/5	50/4.8
17 mm (CR/BV)	74.7/3.9	79.3/4.7	NA	66/5.4	59/3.6	59.9/3.2	85/3.9	62.9/4.2
22 mm (CR/BV)	81.6/3.3	82.8/4	NA	71/4.4	70/3.4	68.6/2.7	89.8/3.3	70.8/3.7
28 mm (CR/BV)	82/2.7	82.1/3.3	NA	85/3.8	61/3.3	79.2/2.2	87.4/3.0	65.1/3.3
37 mm (CR/BV)	84.5/2.2	83.9/2.5	NA	89/3.5	64/3.5	87.4/1.9	89.6/2.2	72.3/1.1
Average lung error	5.6	3.1	NA	5.9	26	3.6	3.5	NA

et al.) was found to be superior to the other scanners (Siemens Biograph 600, GE discovery MI, GE Discovery IQ, Siemens Biograph mMR, and GE Signa PETMRI) compared in the study. On comparing spatial resolution values of uMI550 PETCT system (Singh et al./ present study) with GE Discovery MI scanner Digital PET CT scanner, a percentage increase was noted to be 43.3%/43.3%/85.1% (tan/rad/axial) at 1 cm, 53.3%/61.7%/116.6% (tan/rad/axial) at 10 cm, 38.8%/60.8%/112.9% (tan/rad/axial) at 20 cm respectively.[12] Similarly when comparing the values of spatial resolution of the uMI550 PETCT system (Singh et al.) with the Siemens Biograph Vision 600 Digital PETCT Scanner, it was found that the spatial resolution of the uMI550 PETCT system increased with a percentage increase of 23.3%/16.6%/33.3% (tan/rad/axial) at 1 cm, 30%/35.2%/43.3% (tan/rad/axial) at 10 cm, −2.7%/26%/41.9% (tan/rad/axial) at 20 cm.[15] This superior spatial resolution observed with the digital PETCT uMI550 (Singh et al.) is due to the smaller crystal dimension (2.76 × 2.76 mm) compared to other scanners.[12–16]

Sensitivity

The sensitivity of the uMI550 digital PETCT scanner (Singh et al.) was observed to be comparable to that reported by Chen et al., at centre with PD of 1.06% and slightly lower at 10 cm with a PD of 6.1%. This difference is attributed to differences in operating conditions such as source positioning, random and scatter variation etc.[6] It was observed that the sensitivity of uMI550 (Singh et al.) was higher at both centre and 10 cm (10.35 cps/kBq and 9.74 cps/kBq) compared to analog uMI510 PETCT (8.3 cps/kBq and 8.6 cps/kBq), which is due to the larger crystal length of uMI550 (16.3 mm) than uMI510 (15 mm).[11] The higher sensitivity values result from the higher absorption efficiency with a longer crystal.[6] The sensitivity of Signa PETMR was the highest among all compared models with an axial FOV of 25 cm.[14] According to the literature, this is due to the reduction of the transverse FOV in the scanner from 70 to 60 cm. Due to its high geometric efficiency, this leads to a slightly higher sensitivity.[6,12,14]

Scatter fraction

The scatter fraction was observed at 38.5% which is similar to uMI510.[11] Furthermore, it was found that the scatter fraction values were congruent within PET scanners compared in the study with PD of 4.9% (uMI550, Chen et al.), 6.1% (GE Discovery IQ), 4.3% (GE Discovery MI), 1.2% (Siemens Biograph Vision 600), and proved superior to GE Signa PET MR (PD of 12.4%).[6,12–15]

NECR

The peak NECR values of uMI550 (Singh et al.) proved to be slightly superior than Chen et al. and GE Discovery IQ with PD of

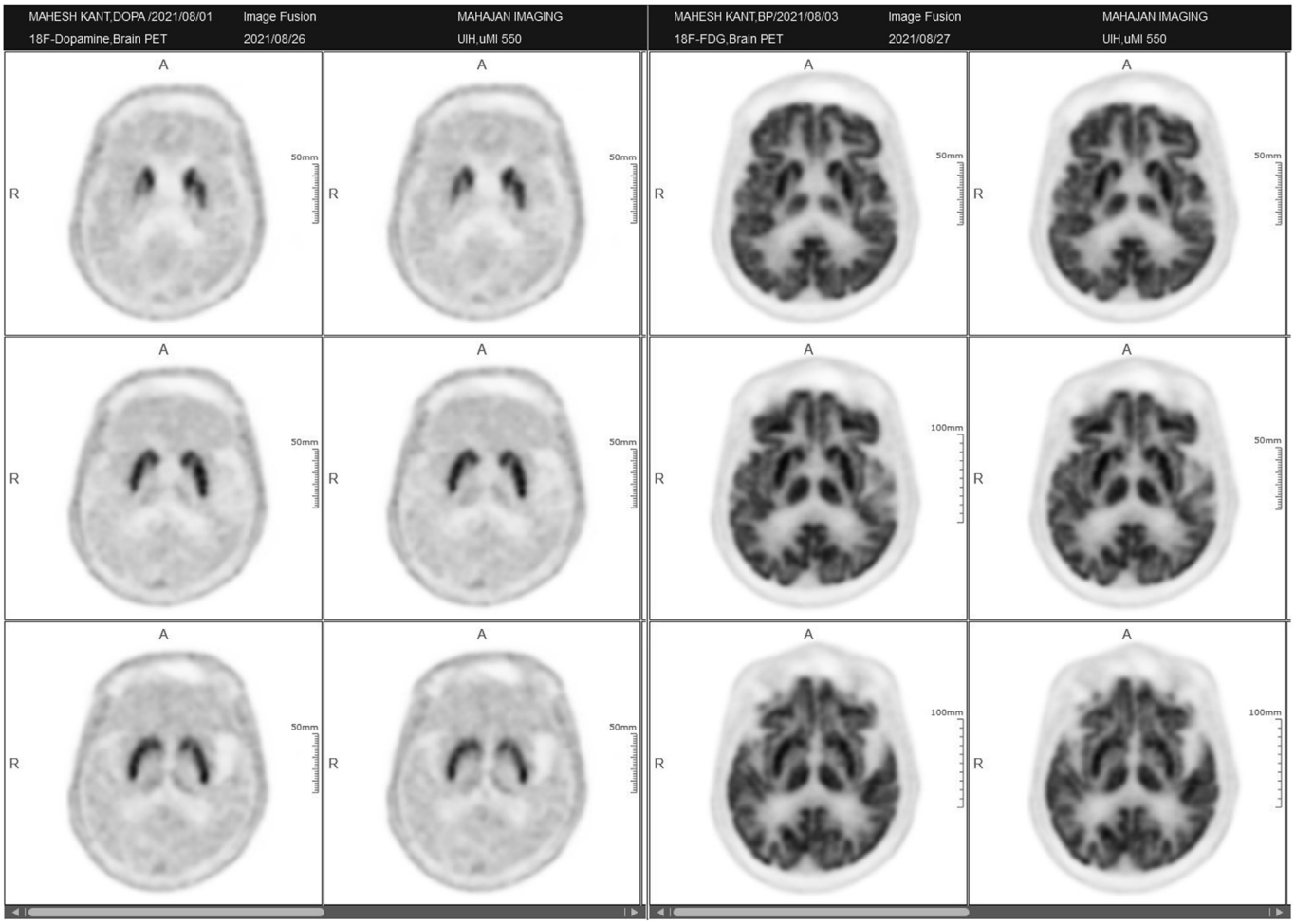

Figure 2. Brain scan of F-DOPA and FDG.

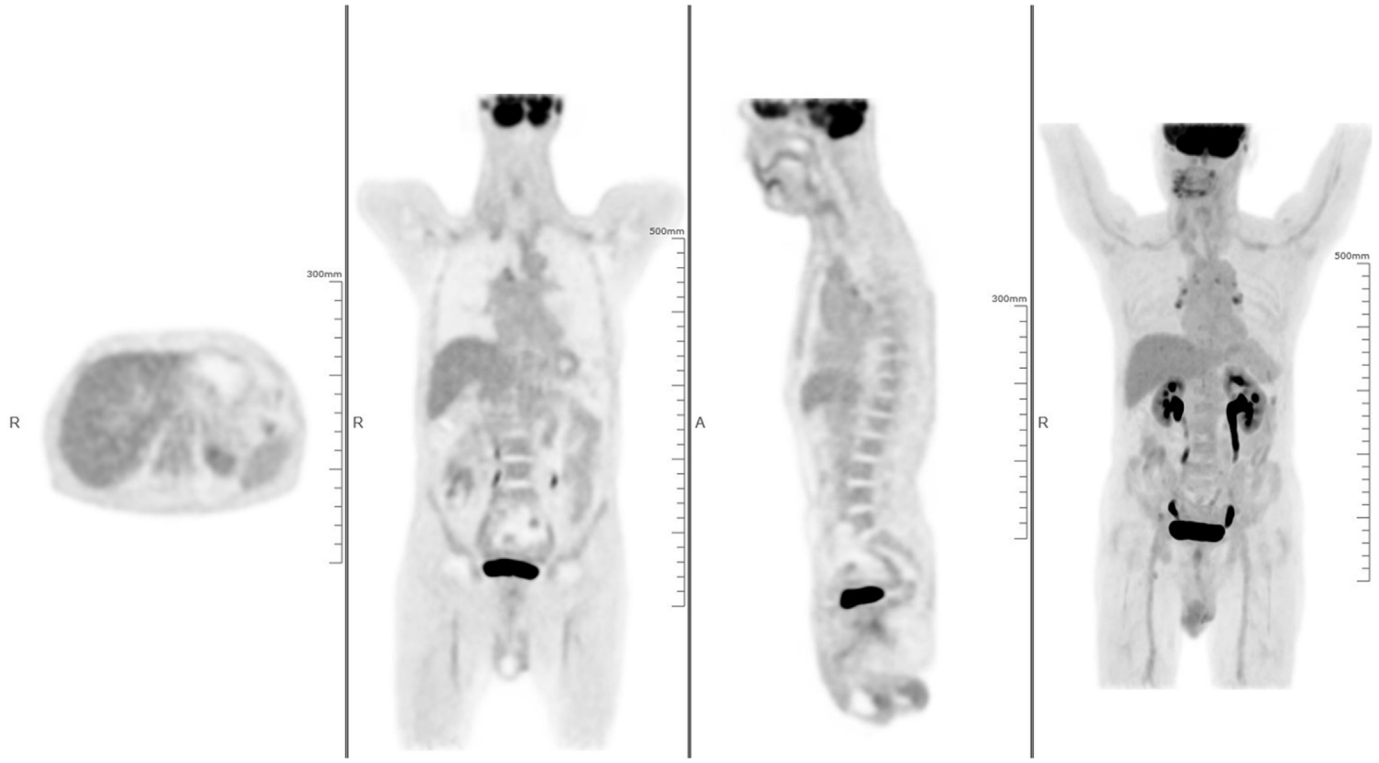

Figure 3. WB FDG Images acquired on uMI550.

4.44% and 5.08% respectively, whereas lower than Siemens Biograph 600, Siemens Biograph mMR, GE discovery MI, and GE Signa PET MRI with PD of 77.9%, 34.3%, 68.7%, and 50.5% respectively. This variation is due to the larger crystal length as shown in Table 4.

Timing resolution

The timing resolution of the uMI550 digital PETCT scanner (Singh et al.) was similar (372ps) to uMI550 (Chen et al.) and proved superior to GE Discovery MI, SiPM based digital PETCT, (381.7 ps) and GE Signa PETMR (386 ps).[12,6] Compared to the PETCT scanner uMI510 (analog) (485 ps), a significantly better timing resolution (372 ps) was observed in the present study, which can be attributed to the improvement in detector technology from PMT to SiPM with digital PETCT.[11] The Siemens Biograph mMR is an avalanche photodiode (APD) based non ToF PETMR scanner and GE Discovery IQ is also a conventional analog PETCT with BGO crystals. These two have no time resolution element.[13,16] The timing resolution of the Siemens Biograph vision 600 (215ps) is superior to the uMI550 scanner in the present study.

Image quality

The image quality was observed to be superior with analog PET scanner i.e., GE Discovery IQ[13] and congruent with digital PETCT scanners uMI550 (Chen et al.), GE Discovery MI, GE Signa PETMR, Siemens Biograph 600, Siemens Biograph mMR as seen in Table 4.[6,12,14–16]

First clinical images

Figs. 2 and 3 show clinical images of brain FDG and 18F-DOPA, as well as FDG whole-body imaging. As illustrated in Fig. 2, the brain images were obtained utilizing a specialized HYPER DLR advanced deep learning-based reconstruction with ToF. It demonstrates that the system can generate high-resolution 512 × 512 matrix PET images at a dosage of ~200 MBq and a scan period of 8 min. Two senior nuclear medicine physicians detected a substantial superiority in image quality in this institution. Deep learning reconstruction in PET with SiPM digital technology enabled to use a lower radiopharmaceutical dose of ~200 MBq, corresponding to a 35%–40% reduction in dosage and 1.5–2 min per bed scan time over the typical PETCT scanner procedure at the existing facility. As a result, image quality and diagnostic confidence have increased (Figs. 2 and 3). This scanner has a 24 cm wide AFOV, allowing it to complete a whole-body scan from the vertex to the mid-thigh in 5 beds. Figs. 2 and 3 illustrates the clear contrast and resolution of the brain image on an FDG and 18F-DOPA scan with a dosage of ~185 MBq and a scan period of 8 min. However, these clinical images provide an overview of the uMI550 digital PETCT scanner's early experience.

Conclusion

The scanner performs excellently across all parameters, owing to the superiority of SiPM-based detector technology. In clinical mode, it produces excellent image quality and adds clinical significance by improving the capability of detecting and differentiating tiny or low contrast lesions without impacting radiopharmaceutical dose or overall scan time.

Funding

No funds, grants, or other support was received.

Ethical approval and informed consent

A small part of present work is an observational study requiring documenting data of clinical images which were obtained as a part

of clinical routine practice in the department. Informed consent was obtained from all individual participants for documenting the clinical images data. Ethics approval was obtained from institutional local ethics committee.

Consent to participate

Informed consent was obtained from all individual participants included in the study.

Consent to publish

The authors affirm that human research participants provided informed consent for publication of the images in figure(s) 2 and 3.

Conflict of interest statement

None.

References

1. Cherry SR, Sorenson JA, Phelps ME. *Physics in nuclear medicine e-Book*. Elsevier Health Sciences; 2012.
2. Vandenberghe S, Moskal P, Karp JS. State of the art in total body PET. *EJNMMI Phys* 2020;**7**(1):1–33.
3. Lecomte R. Novel detector technology for clinical PET. *Eur J Nucl Med Mol Imag* 2009;**36**(1):69–85.
4. Stewart AG, Greene-O'Sullivan E, Herbert DJ, Saveliev V, Quinlan F, Wall L, et al. Study of the properties of new SPM detectors. In: *Semiconductor Photodetectors III*. **6119**. SPIE; 2006. 84–93.
5. Gonzalez-Montoro A, Ullah MN, Levin CS. Advances in detector instrumentation for PET. *J Nucl Med* 2022;**63**(8):1138–44.
6. Chen S, Hu P, Gu Y, Yu H, Shi H. Performance characteristics of the digital uMI 550 PET/CT system according to the NEMA NU2-2018 standard. *EJNMMI Phys* 2020;**7**(1):1–4.
7. Spencer BA, Berg E, Schmall JP, Omidvari N, Leung EK, Abdelhafez YG, et al. Performance evaluation of the uEXPLORER total-body PET/CT scanner based on NEMA NU 2-2018 with additional tests to characterize PET scanners with a long axial field of view. *J Nucl Med* 2021;**62**(6):861–70.
8. National Electrical Manufacturers Association. *NEMA standards publication NU 2–2018: performance measurements of Positron emission tomographs*. Virginia, USA: Rosslyn; 2018.
9. Sharma SD, Prasad R, Shetye B, Rangarajan V, Deshpande D, Shrivastava SK, et al. Whole-body PET acceptance test in 2D and 3D using NEMA NU 2-2001 protocol. *J Med Phys/Assoc Med Phys India* 2007;**32**(4):150.
10. Singh MK, Nanabala R, Muhammed AK, Kottuparamban D, Pokkat J, Nair KS, et al. A cost effective method for the preparation of sodium fluoride [18F] NaF for PET-CT imaging by using an in-house designed module. *Appl Radiat Isot* 2023;**191**:110565.

[11]. Xu B, Liu C, Dong Y, Tang R, Liu Y, Yang H, et al. Performance evaluation of a high-resolution TOF clinical PET/CT. *J Nucl Med* May 2016;**57**(supplement 2): 202.

12. Pan T, Einstein SA, Kappadath SC, Grogg KS, Lois Gomez C, Alessio AM, et al. Performance evaluation of the 5-Ring GE Discovery MI PET/CT system using the national electrical manufacturers association NU 2-2012 Standard. *Med Phys* 2019;**46**(7):3025–33.
13. Reynés-Llompart G, Gámez-Cenzano C, Romero-Zayas I, Rodríguez-Bel L, Vercher-Conejero JL, Martí-Climent JM. Performance characteristics of the whole-body discovery IQ PET/CT system. *J Nucl Med* 2017;**58**(7):1155–61.
14. Grant AM, Deller TW, Khalighi MM, Maramraju SH, Delso G, Levin CS. NEMA NU 2-2012 performance studies for the SiPM-based ToF-PET component of the GE SIGNA PET/MR system. *Med Phys* 2016;**43**(5):2334–43.
15. Reddin JS, Scheuermann JS, Bharkhada D, Smith AM, Casey ME, Conti M, et al. Performance evaluation of the SiPM-based Siemens Biograph vision PET/CT system. In: *2018 Ieee nuclear science symposium and medical imaging conference proceedings (Nss/Mic)*. **10**. IEEE; 2018. 1–5.
16. Delso G, Fürst S, Jakoby B, Ladebeck R, Ganter C, Nekolla SG, et al. Performance measurements of the Siemens mMR integrated whole-body PET/MR scanner. *J Nucl Med* 2011;**52**(12):1914–22.